Desalination and Water Treatment
www.deswater.com

doi:10.5004/dwt.2017.21609

98 (2017) 294–305
December

Adsorption kinetic, equilibrium and thermodynamic study for the removal of Congo Red from aqueous solution

Muhammad Imran Khan[a,b,*], Shagufta Zafar[c,] Muhammad Ali Khan[d], Abdul Rehman Buzdar[e], Prasert Prapamonthon[f]

[a]*School of Chemistry and Material Science, University of Science and Technology of China, Hefei 230026, Anhui, China, email: raoimranishaq@gmail.com*
[b]*Fujian Institute of Research on Structure of Matter, Chinese Academy of Sciences, Fuzhou 350002,Fujian, China*
[c]*Department of Chemistry, The Government Sadiq College Women University, Bahawalpur 63000, Pakistan, email: shg_zf@yahoo.com*
[d]*Institute of Chemical Sciences, Bahauddin Zakariya University, Multan 60000, Pakistan, email: malichem92@fjirsm.ac.cn*
[e]*CSE Department, HITEC University Taxila Cantt 47050, Pakistan, email: buzdar@mail.ustc.edu.cn*
[f]*King Mongkut's Institute of Technology Ladkrabang, Bangkok, Thailand, email: prasert.pr@kmitl.ac.th*

Received 1 July 2017; Accepted 7 November 2017

ABSTRACT

In this study, the adsorption of *Congo red (CR)* dye from aqueous solution onto *cationic polymeric film (BIII)* was investigated at ambient temperature. The effect of operational parameters such as contact time, membrane dosage, initial dye concentration and temperature on the adsorption of *CR* from aqueous solution was studied. Adsorption kinetics has been studied by employing several kinetic models and attained results showed that the adsorption data fitted-well to the pseudo-second-order kinetic model. Nonlinear forms of two parameters and three parameters isotherms were applied on experimental data and the results indicated that the adsorption data fitted well to the various two and three parameters isotherms. Thermodynamic study showed that the adsorption of *CR* onto *cationic polymeric film (BIII)* was an exothermic process.

Keywords: Adsorption; *Congo red*; Cationic *polymeric film*; Nonlinear adsorption isotherms; Thermodynamics

1. Introduction

Dyes are kind of organic compounds that give bright and firm color to other substances. Synthetic dyes usually have a complex aromatic molecular structure, normally formed from benzene, naphthalene, anthracene and xylene etc. [1]. Dyes widely used in textile, paper, plastic, food, and cosmetic industries is an easily recognized pollutant [2]. Decolorizing of textile and manufacturing of wastewater is currently a major problem for environmental managers [3]. Dyes may significantly affect photosynthetic activities in aquatic life due to presence of aromatic metals, chlorides and many others toxins in them [4]. Many of the dyes used in the industries are stable to light and oxidation as well as aerobic digestion [5]. However, dyes usually have synthetic origin and aromatic molecular structure which make them more stable, so that they are not biodegradable and photodegradable, it brings some difficulties for the treatment of these pollutant [6]. Congo red (CR) is benzidine-based anionic diazo dye, this dye is known to metabolize to benzidine a known human carcinogen [7]. There is a crucial requirement for decoloration and removal of dye from industrial effluents.

Several methods have been developed to treat the dye-containing effluents, including biological treatment [8], coagulation/flocculation [9], ozone treatment [10], chemical oxidation [11], membrane filtration [12], ion exchange [13], photocatalysts [14], and adsorption [15]. Among these

*Corresponding author.

methods, adsorption is are liable alternative due to its simplicity, high efficiency, and ease of operation as well as the availability of a wide range of adsorbents. A commonly used adsorbent, *activated carbon* has a high capacity for the removal of dye/organics [16–18]. But some of its disadvantages are the high price of treatment and difficult to regenerate which gives the increase in cost of the wastewater treatment. Thus there is a demand for the other adsorbents which are made up of inexpensive material and locally available such that the adsorption process will become economically viable. Several non-conventional, low cost adsorbents such as organo- attapulgite pellets of trametes versicolor, palm shells, montmorillonite, bentonite, rice hull ash, leaf, and rice husk have been used for the removal of *Congo red* from aqueous solution [16]. Beside these, *fly ash, kaolin*, and *residue sludge* were also used as adsorbents for removal of *Congo red* from aqueous solution [19]. In view of pollutant control at present, it is still indispensible to exploit the new adsorbent materials with high adsorption capacities and removal efficiencies.

Nowadays, almost all the adsorbents developed for the removal of heavy metal ions and dyes rely on the interaction of the target compounds with the functional groups that are present on the surfaces of the adsorbents [20]. Therefore, a large surface area and many adsorption sites of the matrix are essential for adsorption affinity of membranes to remove the contaminants from wastewater, and the specific surface area was one of the most important factors to affect the adsorption capacity of the adsorbents [21–23]. Thus the *ionic polymeric film* become an excellent choice as adsorbent for removal of dye from aqueous solution because it exhibits large surface area for adsorption. Cationic dye *methyl violet 2B* was removed from aqueous solution by two kinds of polymeric films *P81 and CE450* via adsorption process [24]. Similarly *cationic polymeric film* was developed for absorption removal of anionic dye *Cibacron Blue 3GA* from aqueous solution [25]. In our previous work, we have used *cationic polymeric film (EPTAC)* for removal of *Congo red* [26] where as *cationic polymeric films (BI, BIII & DF-120B)* were used for removal of *methyl orange (MO)* dye from the aqueous solution [27].

In the present research, the *cationic polymeric film (BIII)* have been used for removal of anionic dye *Congo red (CR)* from aqueous solution at room temperature. The effect of operational endowments such as, contact time, membrane dosage, initial dye concentration and temperature on the adsorption capacity of *CR* from aqueous solution were investigated. The adsorption kinetics, isotherms and thermodynamics for adsorption of *CR* onto *BIII* was studied.

2. Experimental

2.1. Materials

2.1.1. Adsorbent

The commercial cationic *polymeric film (BIII)* provided by Chemjoy Membrane Co. Ltd, Hefei, Anhui, China was used as adsorbent. It was prepared from blends of PVA and QPPO. It was used without further treatment. The ion exchange capacity (IEC) and water uptake (W_R) of BIII are 0.26 mmol/g and 37.3 % respectively. The adsorption capacities of *CR* for different adsorbents are given in Table 1.

Table 1
Adsorption capacities of *Congo red* dye for different adsorbents

Sr. No.	Adsorbent	Capacity (mg/g)	References
1	*Organo-attapulgite*	189.39	[6]
2	*Cattail root*	38.79	[30]
3	*Bagasse Fly ash*	16.3	[31]
4	*H_2O_2 treated Bagasse fly ash*	7.73	[31]
5	*White kidney beans*	0.135	[32]
6	*Acid activated red mud*	7.087	[33]
7	*Anilinepropylsilica xerogel*	40.86	[34]
8	*Bagasse fly ash*	11.885	[7]
9	*Activated carbons—commercial grade*	0.635	[7]
10	*Activated carbons—laboratory grade*	1.875	[7]
11	*Root of Eichhornia crassipes biomass*	14.49	[35]
12	*Guava leaf-based activated carbon*	47.62	[36]
13	*Silver nanoparticles coated activated carbon beads*	0.47	[37]
14	*Gold nanoparticles coated activated carbon beads*	0.50	[37]
15	*Polymeric film BIII*	160.93	Present study

2.1.2. Adsorbate

Congo red (sodium salt of benzdinediazobis-1-nephthylamine-4-sulphonic acid) is a benzidine-based azo dye and it was used as a adsorbate in this study. The molecular formula of CR is $C_{32}H_{22}N_6Na_2O_6S_2$ and its molecular structure is shown in Fig. 1. It mainly occurs in the effluents discharged from textile, paper, printing, leather industries, etc. [28] and during dyeing operation; about 15% of it ends up in wastewaters [29]. All of the reagents were of analytical grade and deionized water was used throughout the experiments.

2.2. Adsorption

Adsorption measurements were carried by batch mode as reported in the literature [16]. In a typical experiment, batch adsorption of *CR* was carried out by immersing known amount of adsorbent (*Polymeric film*) into 40 ml of dye aqueous solutions of known concentration at room temperature. The flasks were shaked at a constant speed of 120 rpm. At predetermined time, the flasks were withdrawn from the shaker and residual dye concentration in the reaction mixture was determined by measuring the absorbance of the supernatant by UV/VIS spectrophotometer (UV-2550, SHIMADZU) at the wavelength ($\lambda_{max.}$= 490 nm for *Congo red*) that corresponds to the maximum absorbance of the sample. Dye concentration in the reaction mixture was calculated from the calibration curve. Adsorption experiments were conducted by varying contact time, adsorbent dose, initial dye concentration and temperature under the

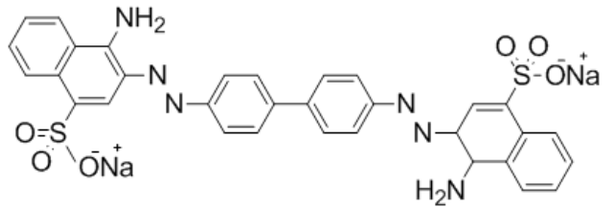

Fig. 1. Chemical structure of Congo Red (CR) dye.

aspect of adsorption kinetic, isotherm and thermodynamic study. The amount of *CR* adsorbed onto *BIII* at time t, was calculated by Eq. (1).

$$q_t = \frac{C_o - C_t}{W} \times V \quad (1)$$

where C_o and C_t are the concentration of *CR* at initial state and at time t respectively. Similarly *V* and *W* are volume of *CR* aqueous solution and weight of membrane respectively.

2.3. FTIR spectra analysis

FTIR spectra of dried *polymeric film* were recorded by using the technique attenuated total reflectance (ATR) with FTIR spectrometer (Vector 22, Bruker) having resolution of 2 cm^{-1} in a spectral range of 4000–400 cm^{-1}.

3. Results and discussion

3.1. FTIR spectra analysis

Fig. 2 shows the FTIR spectra of *polymeric film (BIII)* before and after the adsorption of *CR* dye. Before adsorption of *CR* dye, the peak observed in the range of 2800–3000 cm^{-1} for *polymeric film* corresponds to $–CH_3$ stretching from the PPO back bone. The bands in the range of 1446 cm^{-1} are due to of stretching of –CH groups (*V* and δ) [38]. The band in region of 1600–1620 cm^{-1} is due to stretching vibration of C-N group [39,40]. The broad peaks in the range of 3050–3600 cm^{-1} is due to the presence of –OH groups. The adsorption peaks of symmetrical and asymmetrical stretching vibration of C-O are at 1200 cm^{-1} and 1306 cm^{-1} and those of phenyl group at 1470 cm^{-1} and 1600 cm^{-1} respectively [27].

After the adsorption of *CR* dye onto *polymeric film* surface, some changes were observed in the FTIR spectra. The band in the range of 1320 cm^{-1} is due to the stretching of –S = O group representing the successful adsorption of *CR* dye onto the *polymeric film* surface. The intensity of C-N band at 1600 cm^{-1} is found to be decreased after the adsorption of *CR* onto *polymeric film*. It indicates the successful adsorption CR onto *BIII*. Moreover, the weak band at 1037 cm^{-1} corresponds to the –N=N– stretching vibration [27,41]. This proves the successful adsorption of *CR* onto *BIII* surface.

3.2. Effect of operational parameters

Herein, the effect of operational parameters namely contacts time, adsorbent dosage, initial dye concentration and temperature on the removal of *CR* dye from aqueous solution has been discussed. The detail is given below

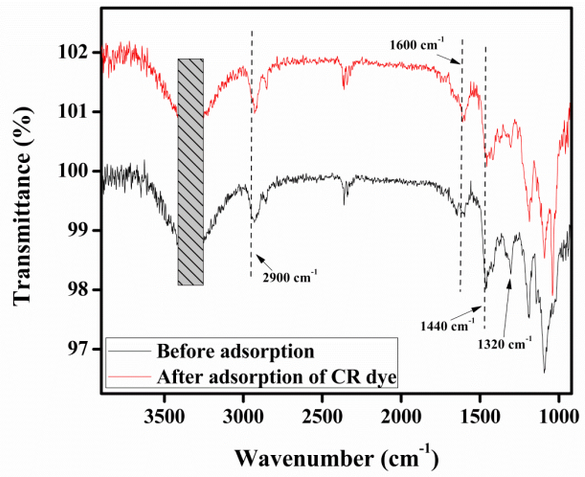

Fig. 2. FITR Spectra of BIII before and after adsorption of CR dye.

3.2.1. Effect of contact time

The effect of contact time on the adsorption of *CR* was studied keeping the shaking speed (120 rpm), concentration of adsorbate (50 mg/L), amount of adsorbent (0.1 g) constant at ambient temperature. The adsorption of *CR* is found to be increased with contact time as represented in Fig. 3 and equilibrium was reached in 24 h and this optimum contact time was used for further experiments. The plot shows that the removal of *CR* was rapid in the initial stage due to large number of available vacant sites on the surface of *Polymeric film* during the initial stage. Similar results have been previously reported in the literature for dye removal [42]. The removal of dye is found to be very fast at the initial stage of contact time but slowed down with the passage of time. Kinetic experiments clearly indicated that the adsorption of *CR* onto *BIII* followed three-step processes, a rapid initial adsorption followed by a period of slower uptake of *CR* and finally no significant uptake. The first step is attributed to the instantaneous utilisation of the most readily available active sites onto the adsorbent surface (bulk diffusion). Second step, exhibiting the additional adsorption is attributed to the diffusion of the adsorbate from the surface film into the macro-pores of the adsorbent (pore diffusion or intra-particle diffusion) stimulating further movement of *CR* molecules from the liquid phase onto adsorbent surface. The last stage is an equilibrium stage [43]. The rapid kinetics has significant practical importance, as it facilitates smaller reactor volumes, ensuring high efficiency and economy [44,45].

3.2.2. Effect of membrane dosage

The effect of adsorbent dosage is crucial to investigate the maximum adsorption with small possible amount of adsorbent. The effect of the *polymeric film* dosage on the

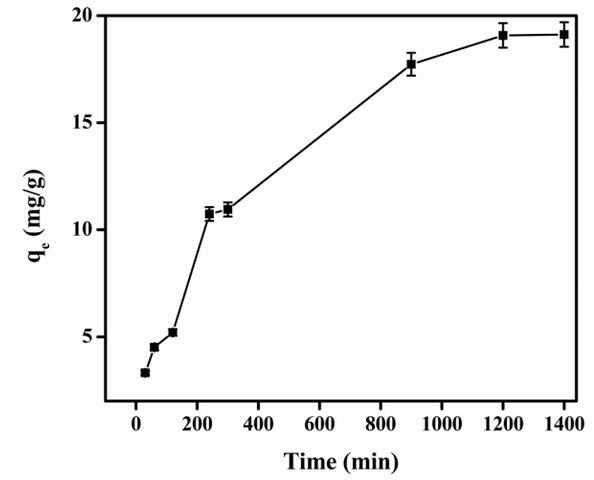

Fig. 3. Effect of contact time on the adsorption of CR onto BIII.

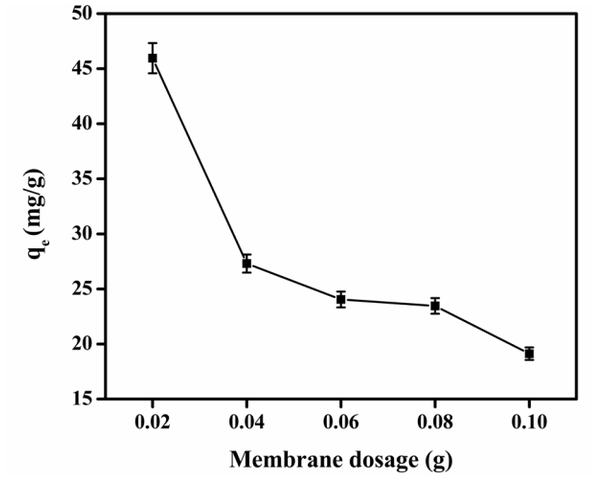

Fig. 4. Effect of membrane dosage on the adsorption of CR onto BIII.

adsorption capacity of *CR* was studied keeping the other factors such as contact time, initial dye concentration, shaking speed and temperature constant. The percentage adsorption of C*R* is found to be increased with increasing the amount of *polymeric film* dosage and results are shown in Fig. 4. The removal of *CR* dyes is found to be increased from 45.95% to 95.60% with increasing the dosage from 0.02 g to 0.1 g because number of available active sites increases with increasing the *Polymeric film* dosage. Similarly results have been previously reported in the literature [30]. However, further increment in the adsorbent dosage did not give any significant changes in the percentage removal and this could be due to the saturation of binding sites [46].

3.2.3. Effect of initial dye concentration

The effect of initial concentration of dye on the adsorption of *CR* was studied keeping the other endowments such contact time, film dosage, shaking speed and temperature constant. The adsorption capacity of *CR* is found to be increased with increasing the initial concentration of dye as shown in Fig. 5. It gives useful driving forces to overcome the resistance of mass transfer from aqueous phase to the solid phase. The increase in dye concentration also increases the interaction between dye and adsorbent. The adsorption capacity (q_e) of *CR* onto *BIII* increases with the same proportion as the initial dye concentration increases. This behavior is due to the concentration gradient between *CR* dye solution and *cationic film* surface and mass transfer driving forces are higher at high *CR* concentration [47,48].

3.2.4. Effect of temperature

The effect of temperature on the adsorption of *CR* was studied keeping the contact time, film dosage, stirring speed, solution volume and concentration (50 mg/L) constant and results are depicted in Fig. 6. The adsorption capacity of *CR* is found to be decreased from 19.12 to 15.53 mg/g with increasing the temperature from 303 K to 323 K. It shows that the adsorption of *CR* onto *BIII* is an exothermic process as it decreases at high temperature.

3.3. Adsorption kinetics

Many adsorption models were employed to study the controlling mechanism of adsorption process such as chemical reaction and diffusion control

3.3.1. Pseudo-first-order model

The linearized form of the Lagergren pseudo-first-order rate equation is given by [49].

$$loq(q_e - q_t) = \log q_e - \frac{K_1 t}{2.303} \tag{2}$$

where q_e and q_t is the adsorbed amount of dye at equilibrium and time t repectively and k_1 (/min) is the rate constant of pseudo-first-order adsorption model. The plot of $\log(q_e - q_t)$ vs. time for adsorption of *CR* onto *BIII* is shown in Fig. 7. The values of parameters (k_1 and q_e) obtained from slope and intercept are given in Table 2. These plots are linear, however the linearity of these curves does not necessarily assure the mechanism due to the inherent disadvantage of correctly estimating equilibrium adsorption capacity [50]. The correlation cofficient (R^2) value for adsorption of *CR* onto *BIII* was 0.892. Moreover, there is a large difference between experimental adsorption capacity ($q_{e,exp}$) and calculated adsorption capacity values ($q_{e,cal}$), therefore the pseudo-first-order model does not explain the rate process.

3.3.2. Pseudo-second-order model

The linearized form of pseudo-second kinetic model is expressed as [51]

$$\frac{t}{q_t} = \frac{1}{k_2 q_e^2} + \frac{t}{q_e} \tag{3}$$

where k_2 (g/mg·min) is the rate constant of pseudo-second-order model. The plot of t/q_t vs. t for pseudo-second-

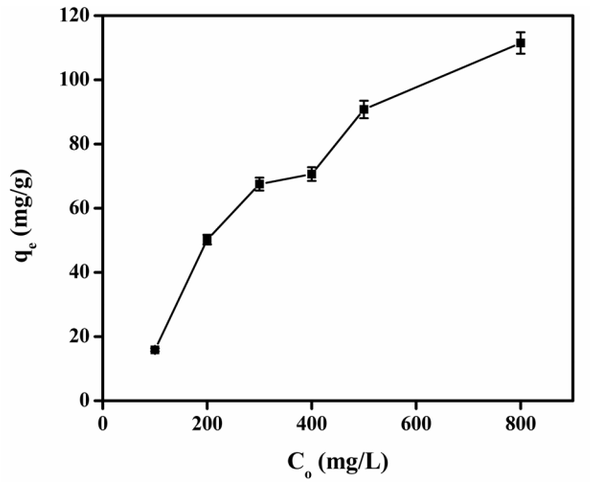

Fig. 5. Effect of initial dye concentration on the adsorption of CR onto BIII.

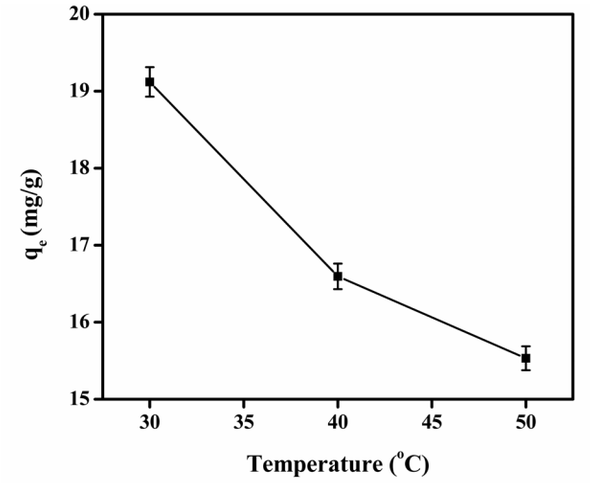

Fig. 6. Effect of initial dye concentration on the adsorption of CR onto BIII.

order model is depicted in Fig. 8. The value of adsorption capacity (q_e) can be measured from slope of plot and given in Table 2. This value is in good agreement with the experimental value (19.12 mg/g). The value of correlation cofficient is ($R^2 > 0.99$) which indicates that the experimental data fitted well to the pseudo-second-order model.

3.3.3. Elovich model

The most interesting model to describe the activated chemisorption is the Elovich equation [52].

$$q_t = \frac{1}{\beta}\ln(\alpha\beta) + \frac{1}{\beta}\ln t \quad (4)$$

where α (mg/g·min) and β (g/mg) are constant. The parameter α is considered as initial adsorption rate (mg/g·min) and β is related to the extent of surface coverage and activation energy for the chemisorption. The graphical representation of Elovich model is given in Fig. 9. The values of α and β are measured from intercept and slope of plot and are given in Table 2. The value of correlation coefficient (R^2) was 0.953 lower than that of pseudo-second-order model.

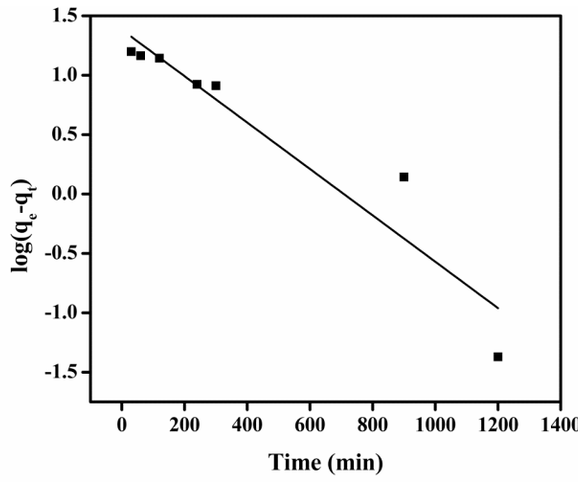

Fig. 7. Pseudo-first-order kinetics for adsorption of CR on BIII.

Table 2
Pseudo-first-order, pseudo-second-order and Elovich model rate constants (q_e: mg/g; k_1: (/min); k_2: g/mg·min; α: mg/g·min; β: g/mg)

Pseudo-first-order				Pseudo-second-order			Elovich model		
$q_{e(exp)}$	$q_{e\,(cal)}$	$k_1\times10^{-3}$	R^2	q_e	$k_2\times10^{-4}$	R_2	α	β	R^2
19.12	23.98	4.38	0.892	22.50	1.83	0.993	0.20	0.22	0.953

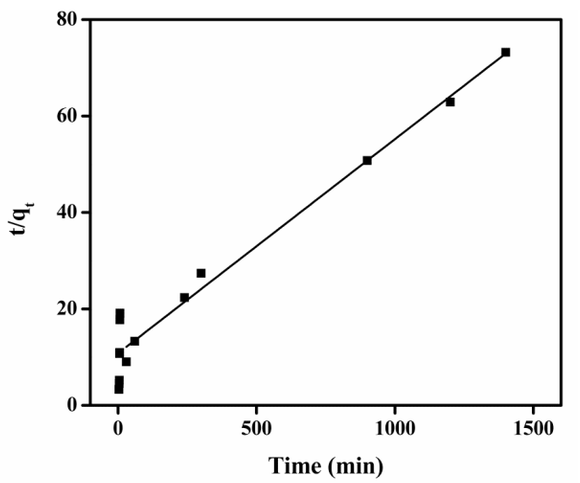

Fig. 8. Pseudo-second-order kinetics for adsorption of CR onto BIII.

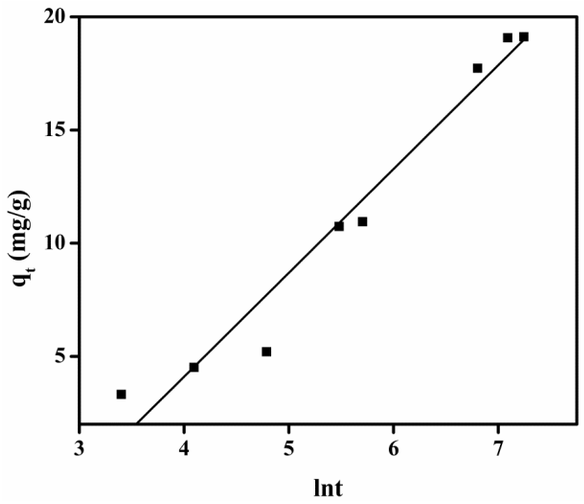

Fig. 9. Elovich model for adsorption of CR onto BIII.

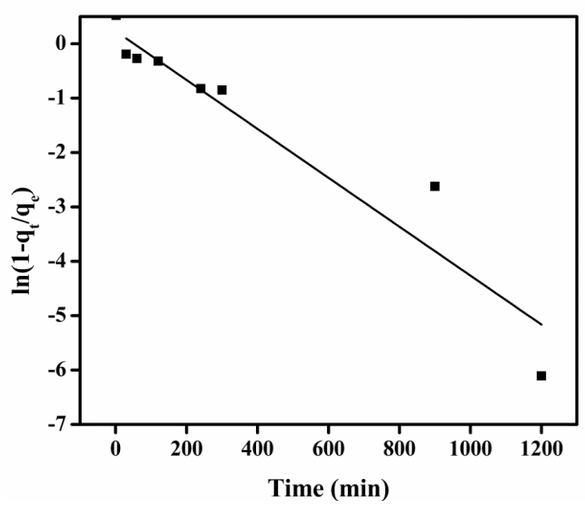

Fig. 10. Liquid film diffusion model for adsorption of CR onto BIII.

3.3.4. Liquid film diffusion model

The migration of dye through liquid film from bulk solution to the exterior surface of adsorption sites may play an important role in determining the adsorption rate. For the prediction of potential rate-controlling step, the data of *CR* adsorption onto *BIII* was investigated utilizing liquid film diffusion model. The liquid film model is expressed as [53].

$$Ln(1-\frac{q_t}{q_e}) = -K_{fd}t \quad (5)$$

where K_{fd} is liquid film diffusion rate constant. The plot of ln $(1–q_t/q_e)$ vs time is a straight line for liquid film model and is represented in Fig. 10. The value of K_{fd} was calculated from slope of the linear plot and is given in Table 3. The value of correlation coefficient (R^2) was 0.892 for the adsorption of *CR* onto *BIII* which is lower than pseudo-second-order model. The inability of the plot to pass through the origin (i.e., zero intercept) shows that the Liquid film model was not only the rate determining step in the adsorption of *CR* onto *BIII* but there also involves other mechanisms. It indicates that the liquid film diffusion model cannot be sufficient to explain the experimental data and other models are also required for explanation of adsorption data.

3.3.5.Modified Freundlich equation

The modified Freundlich equation was originally developed by Kuo and Lotse [54].

$$q_t = kC_o t^{1/m} \quad (6)$$

where q_t is the amount of adsorbed dye (mg/g) at time t, k is apparent adsorption rate constant (L/g·min), C_o is the initial dye concentration (mg/L), t is the contact time (min) and m is the Kuo-Lotse constant. The values of k and m were used to evaluate the effect of dye surface loading and ionic strength on the adsorption process. Linear form of modified Freundlich equation is given as:

$$\ln q_t = \ln(kC_o) + \frac{1}{m}\ln t \quad (7)$$

The graphical representation of modified Freundlich equation is given in Fig. 11. The parameters m and k were obtained from the slope and intercept of plot of ln t Vs. ln q_t and are given in Table 3. The value of correlation coefficient for adsorption of *CR* onto *BIII* is 0.967.

Table 3
Liquid film diffusion model, modified Freunlich equation and Bangham equation rate. Constant (k_{fd}: (/min); k : L/g·min; k_o: mL/g/L)

Liquid film diffusion model			Modified Freundlich equation			Bangham equation		
$k_{fd}\times10^{-3}$	C_{fd}	R^2	m	k	R^2	k_o	α	R_2
4.45	0.23	0.892	2.10	0.013	0.967	0.50	0.49	0.967

3.3.6. Bangham equation

Bangham equation [55] is given as

$$\log\log\left(\frac{C_o}{C_o - q_t m}\right) = \log\left(\frac{k_o m}{2.303V}\right) + \alpha\log t \quad (8)$$

where C_o is the initial concentration of dye solution (mg/L), V is volume of solution (mL), q_t is amount of dye adsorbed (mg/g) at time t, m is weight of adsorbent used (g/L). α (<1) and k_o (mL/(g/L) are constants. The plot of log log(C_o/ $C_o - q_t$ m) vs. log t for adsorption of *CR* onto *BIII* is given in Fig. 12. The values of α and m were obtained from slope and intercept of straight line and are given in Table 3. The double logarithmic plot did not give linear curves for *CR* adsorption onto *BIII* representing that the diffusion of

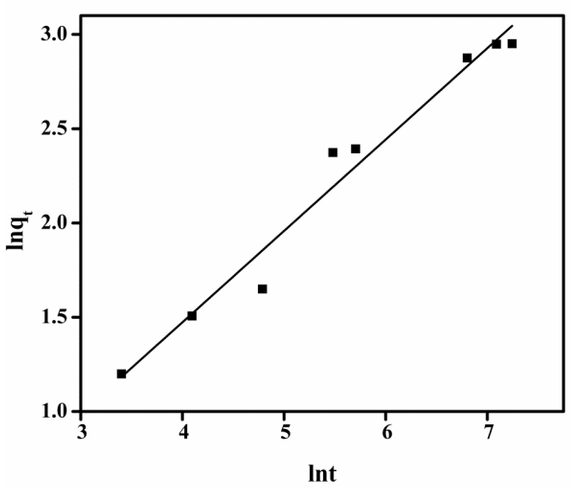

Fig. 11. Modified Freundlich equation plot between ln t vs ln q_t for adsorption of CR onto BIII.

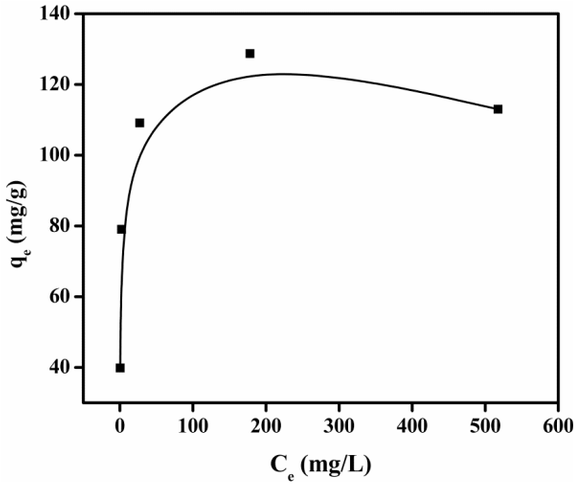

Fig. 13. Adsorption isotherm for adsorption of CR onto BIII.

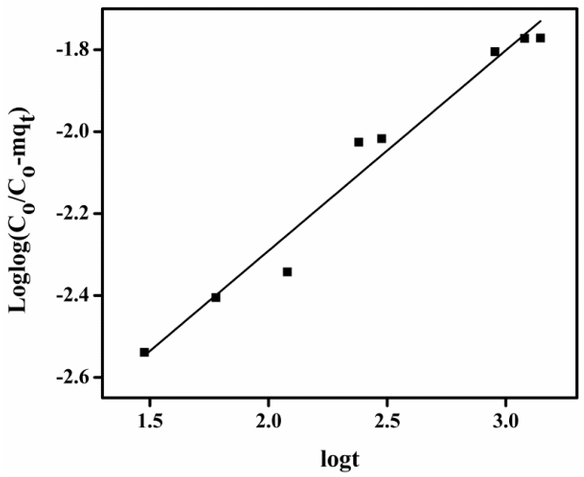

Fig. 12. Bangham equation plot between log t vs log log (C_o/C_o – mq_t) for adsorption of CR onto BIII.

adsorbate into pores of the sorbent is not the only rate controlling step [56,57]. It may be that both film and pore diffusion were crucial to different extent in the adsorption of *CR* from aqueous solution.

3.4. Adsorption isotherms

Adsorption isotherms provide important informations on the adsorption capacity of the adsorbents and the type of adsorbent-adsorbate interaction. The adsorption isotherms are drawn between the quantity of dye adsorbed per gram of film"q_e" and the quantity of dye left in equilibrium solution C_e and is shown in Fig. 13. The adsorption isotherm shows that the adsorption capacity "q_e" increases with the concentration of dyes and the distribution of molecules between solid and liquid phases at equilibrium state. The analysis of isotherm data by fitting the data to different isotherm models is an important step in finding the most suitable model that can be used to describe the adsorption process [58].

There are several isotherm model to describe the isotherm data. Langmuir, Freundlich Temkin and Dubinin-Radushkevich (D-R) are two parameters isotherm models and Redlich-Peterson, Hill, SIPS and Toth are three parameters isotherms which are used to reveal the experimental data of *CR* adsorption onto *BIII*. For adsorption isotherm's parameters determination, the nonlinear method is preferred to the linear one. The linear method assumes that the scattered points around the line follow a Gaussian distribution and that the distribution error is the same at every value of the abscissa. This is virtually impossible with equilibrium isotherm models, as most of the isotherm models are nonlinear. Thus the error distribution will alter after transforming the data into a linear form [59,60]. All the model parameters were evaluated by non-linear regression using Igor Pro. Wave Matrices 6.2.1 software [61]. The nonlinear chi-square test (χ^2) is a statistical tool required for the best fit of an adsorption system and its large value indicates the variation while its small value shows similarities of the experimental data [62].

3.4.1. Two parameters adsorption isotherms

Langmuir, Freunlich, Temkin and Dubinin-Radush kevich (D-R) isotherms are two parameters isotherms models.

Langmuir model depends upon the maximum adsorption coincides to the saturated monolayer of liquid (adsorbate) molecules on the solid (adsorbent) surface. The nonlinear form of Langmuir model is given as follows [63].

$$q_e = \frac{Q_m k_L C_e}{1 + k_L C_e} \tag{9}$$

where K_L is Langmuir constant (L/mol) and Q_m is Langmuir monolayer adsorption capacity (mol/g), C_e is supernatant concentration at equilibrium state of the system (mol/L), and q_e is the amount of dye adsorbed at equilibrium state

of system (mol/g). The nonlinear plot of Langmuir model is shown in Fig. 14. The values of Q_m and K_L are given in Table 4. The chi-square test (χ^2) value is very small indicating that the adsorption of *CR* onto *BIII* fitted well to the Langmuir model. Moreover, the value of Q_m (2.31×10^{-4} mol/g) is close to the experimental value (6.82×10^{-4} mol/g).

The widely used Freundlich model is an empirical relation used to explain the heterogeneous system. The Freundlich isotherm model is expressed as [64].

$$q_e = K_f C_e^{1/n} \tag{10}$$

where K_f and n are Freundlich constant. The values of n and K_f are calculated from nonlinear plot of Freunlich isotherms and given Table 4. The chi-square test (χ^2) is 1.65×10^{-9} showing that the adsorption data followed the Freundlich model. The value of Freundlich constant n decides the favourability of adsorption process. If the value of n is in range from 1 to 10, the adsorption process is favourable. The value of n for *CR* adsorption onto *BIII* was 1.740 indicating the favourable adsorption process.

The Temkin isotherm assumes that the heat of adsorption of all the molecules decrease linearly with the coverage of the molecules due to the adsorbate-adsorbate repulsion and the adsorption of adsorbate is uniformly distributed and that the fall in the heat of adsorption is linear rather than logarithmic [65]. It is expressed as

$$q_e = \frac{RT}{b_T} \ln\left(a_T C_e\right) \tag{11}$$

where T is absolute temperature (K) and R is gas constant (8.31 J/mol·K) and b_T is related to the heat of adsorption and a_T is equilibrium binding constant coinciding to the maximum binding energy. The nonlinear plot of Temkin adsorption isotherm model is given Fig. 14. The value of b_T and a_T were determined and are given in Table 4. The Chi-square for Temkin isotherm is small representing that the adsorption of *CR* onto *BIII* followed the Temkin model.

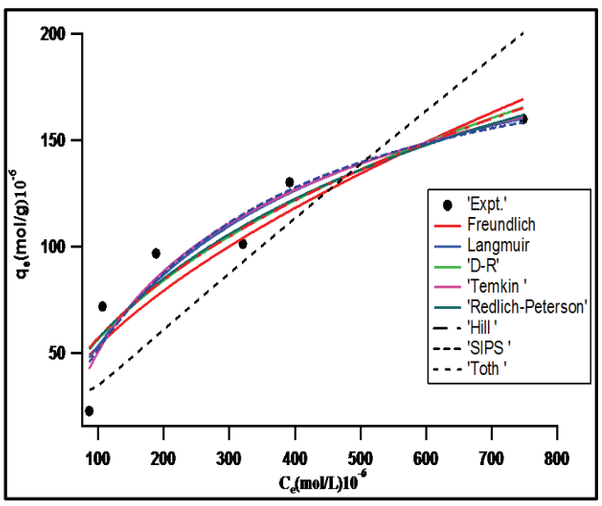

Fig. 14. Nonlinear plots of different adsorption isotherms for the adsorption on CR on BIII.

The adsorption experimental data was applied to the Dubinin-Redushkevich (D-R) model to distinguish between physical and chemical adsorption [65]. The nonlinear D-R model is expressed as

$$q_e = C_m \exp\left(-\beta\varepsilon^2\right) \tag{12}$$

where β is the activity coefficient related to mean sorption energy and ε is the polanyi potential that is given as

$$\epsilon = RTln\left(1+\frac{1}{C_e}\right) \tag{13}$$

where R is the universal gas constant (kJ/mol) and T is the absolute temperature (K). β is related to the mean adsorption energy by the following expression

$$E = \frac{1}{\sqrt{2\beta}} \tag{14}$$

The nonlinear plot of D-R isotherm is given in Fig.14. The mean adsorption energy (E) in the D-R isotherm can act as a rule to differentiate chemical and physical adsorption [66]. For magnitude of E between 8 KJ/mol and 16 KJ/mol, the adsorption process followed chemical ion exchange, and values of E below 8 KJ/mol were the characteristic of physical adsorption process [67]. The value of E for *CR* adsorption onto *BIII* is 9.604 kJ/mol indicating that the *CR* adsorption onto *BIII* followed chemical adsorption.

Table 4
Adsorption isotherm parameters of *CR* adsorption on *BIII* by nonlinear method

Isotherm	Parameter			χ^2
Two parameters isotherms				
Freundlich	K_f		n	1.65×10^{-9}
	1.05×10^{-2}		1.740	
Langmuir	Q_m		K_L	1.22×10^{-9}
	2.31×10^{-4}		3007	
D-R	C_m		B	1.43×10^{-9}
	8.97×10^{-4}		5.42×10^{-3}	
	E = 9.604 kJ mol^{-1}			
Temkin	a_T		b_T	1.04×10^{-9}
	25065		44607	
Three parameters isotherms				
Redlich-Peterson	K_{RP}	a_{RP}	G	1.39×10^{-9}
	0.264	0.0673	0.726	
Hill	q_h	n_h	K_h	1.46×10^{-9}
	6.3×10^{-4}	0.630	0.0302	
SIPS	a_s	*beta*	K_s	1.18×10^{-9}
	12406	1.141	2.553	
Toth	a_T	K_T	T	4.95×10^{-9}
	-7.95×10^{-5}	0.153	13.127	

3.4.2. Three parameters adsorption isotherms

The experimental data of *CR* adsorption onto *BIII* was also analyzed using the three parameter isotherm models namely, Redlich-Peterson, Hill, Sips and Toth. The three parameter models represent the adsorption capacity as characteristic function of the equilibrium concentration C_e and are empirical in nature [68].

Redlich–Peterson is a hybrid isotherm containing both Langmuir and Freundlich isotherms elements which describes equilibrium on homogeneous and heterogeneous surfaces and multilayer adsorption. The Redlich–Peterson (R-P) isotherm [69] contains three parameters, a_{RP}, K_{RP} and g. Non-linear form of R-P isotherm is represented by the equation:

$$q_e = \frac{K_{RP} C_e}{1 + a_{RP} C_e^{\,g}} \tag{15}$$

This equation may be used to represent the adsorption equilibrium over a wide concentration range of dye molecules. The exponent g lies between 0 and 1. When β = 1, the R-P equation becomes the Langmuir equation, and when β = 0, it becomes the Henry's law [70]. From Fig. 14, it is indicated that the experimental data follow R-P model as χ^2 has small values for *CR* adsorption onto *BIII*. The calculated R-P model parameters are given in Table 4.

Hill model assumes that adsorption is a cooperative phenomenon, with the ligand binding capability at one site on the macromolecule [71]. The nonlinear form of Hill adsorption isotherm can be expressed as:

$$q_e = \frac{q_H C_e^{\,n_H}}{k_H + C_e^{\,n_H}} \tag{16}$$

The plot of Hill model is presented in Fig. 14 and the calculated parameters are given in Table. 4. The chi-square values of Hill model is small confirming the adsorption of *CR* onto *BIII* can be defined by Hill model.

Sips isotherm is a combined form of Langmuir and Freunlich expressions derived for predicting the heterogeneous adsorption process [72]. Non-linear form of Sips isotherm is represented by:

$$q_e = \frac{K_S C_e^{\,\beta}}{1 + a_S C_e^{\,\beta}} \tag{17}$$

At low adsorbate concentrations, the Sips isotherm does not obey Henry's law and reduces to the Freunlich isotherm. At high adsorbate concentrations, it follows Langmuir isotherm. The values of Sips parameters evaluated from Fig. 14 are given in Table 4. The Sips equation obeys the equilibrium data adequately as value of χ^2 was too low. The experimental data is more of a Langmuir form rather than that of Freunlich as the exponent α value is about 1.1. The low vales of χ^2 indicated that the experimental data is well explained by Sips model.

Toth isotherm is useful in describing the adsorption in heterogeneous systems. It assumes that the most sites have adsorption energy less than the mean value. Toth isotherms parameters were evaluated from equation:

$$q_e = \frac{K_T C_e}{\left(a_T + C_e\right)^{1/t}} \tag{18}$$

which is a non-linear forms of Toth adsorption isotherm and its plot is given in Fig. 14. The calculated values of Toth parameters are given in Table 4. The low value of χ^2 indicated that experimental data follow by Toth model.

3.5. Adsorption thermodynamics

Thermodynamic endowments represent the feasibility and spontaneity of the adsorption process. The parameters including change in Gibb's free energy (ΔG°), enthalpy (ΔH°) and entropy (ΔS°) were measured from given relations

$$\ln Kc = \frac{\Delta S^o}{R} - \frac{\Delta H^o}{RT} \tag{19}$$

$$K_c = \frac{C_a}{C_e} \tag{20}$$

$$\Delta G^o = \Delta H^o - T\Delta S^o \tag{21}$$

where K_c, C_a, C_e, R, T are the equilibrium constant, amount of dye (mol/L) adsorbed on the adsorbent per litre (L) of the solution at equilibrium, equilibrium concentration (mol/L) of dye in solution, general gas constant (8.31 J/mol·K) and absolute temperature (K) respectively. Similarly ΔG°, ΔH° and ΔS° are the change in Gibb's free energy (KJ/mol), enthalpy (KJ/mol) and entropy (J/mol·K) respectively. The plots of ln K_c verses 1/T for the adsorption of *CR* onto *BIII* is shown in Fig. 15. The adsorption enthalpy (ΔH°) and entropy (ΔS°) were measured from slope and intercept of Fig. 15 and are given in Table 5. The values of Gibb's free energy (ΔG°) are found to be positive as represented in Table 5. It might be because of intraction between adsorbent and adsorbate, with unbalanced competition imputed to heterogeneity of membrane surface and system got energy from external source at higher temperatures which is similar to our previous work [26,73]. The nagative value of enthalpy (ΔH°) indicates that the adsorption of *CR* onto *BIII* is an exothermic process. Similarly the negative value of entropy (ΔS°) shows the decrease in randomness at the dye-film interface during the adsorption of *CR* onto *BIII*.

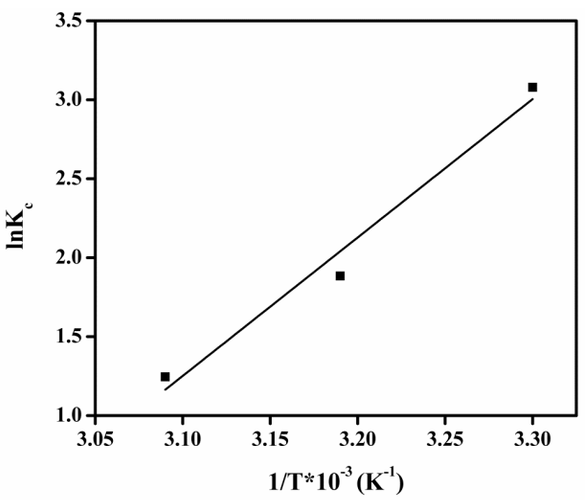

Fig. 15. Plot of 1/T vs ln K_c for adsorption of CR onto BIII.

Table 5
Thermodynamic parameters for adsorption of *CR* onto *BIII*

		ΔG° (KJ/mol)		
ΔH° (KJ/mol)	ΔS° (J/mol)	303K	313K	323K
–72.87	–215.40	6.51	6.73	6.95

4. Conclusions

This studies revealed that the *cationic polymeric film (BIII)* is useful for removal of *congo red (CR)* dye from aqueous solution at room temperature. The adsorption of *CR* from aqueous solution is affected by several factors namely contact time, amount of adsorbent and initial dye concentration. The percentage removal of *CR* dye is enhanced with contact time and amount of adsorbent. The adsorption kinetics study indicated that the adsorption of *CR* onto *BIII* follows the pseudo-second-order kinetic model. The experimental adsorption data was applied to two and three parameters adsorption isotherm models namely Langmuir, Freundlich, Temkin, Dubinin-Radushkevich (D-R), Redlich-Peterson, Hill, Sips and Toth and fitted well to all these isotherms but best obeyed by Langmuir isotherm model. The negative value of enthalpy (ΔH°) shows that adsorption of *CR* onto *BIII* is an exothermic process. The present study showed that the *cationic polymeric film (BIII)* could be used as an excellent adsorbent for *CR* dye from aqueous solution.

Symbols

IEC — Ion exchange capacity (mmol/g)
W_R — Water uptake (%)
C_o — Initial concentration of dye (mg/L)
C_t — Concentration of dye at time t (mg/L)
W — Weight of adsorbent (g)
V — Volume of adsorbate (dm^3)
k_1 — Rate constant of pseudo-first-order model (/min)
k_2 — Rate constant of pseudo-second-order model (g/mg·min)
α — Initial sorption rate (mg/g·min)
β — Extent of surface coverage and activation energy for the chemisorption (g/mg).
K_{fd} — Liquid film diffusion rate constant
k — Apparent adsorption rate constant (L/g·min)
m — Kuo-Lotse constant.
b — Langmuir constant (L/mg)
q_m — Langmuir monolayes adsorption capacity (mg/g)
K_f — Freunlich constant
T — Absolute temperature (K)
R — Gas constant (8.31 J/mol·K)
b_T — Heat of adsorption (J/mol)
A_T — Equilibrium binding constant coinciding to the maximum binding energy (L/mg)
$\Delta G°$ — Change in Gibb's energy
$\Delta S°$ — Change in entropy
$\Delta H°$ — Change in enthalpy

Acknowledgement

The authors are highly thankful to the CAS-TWAS President's fellowship for financial support.

References

[1] R. Gong, Y. Sun, J. Chen, H. Liu, C. Yang, Effect of chemical modification on dye adsorption capacity of peanut hull, Dyes Pigm., 67 (2005) 175–181.
[2] S.T. Ong, C.K. Lee, Z. Zainal, Removal of basic and reactive dyes using ethylenediamine modified rice hull, Bioresour. Technol., 98 (2007) 2792–2799.
[3] Y. Ho, C. Chiang, Sorption studies of acid dye by mixed sorbents, Adsorption 7 (2001) 139–147.
[4] B. Hameed, M. El-Khaiary, Equilibrium, kinetics and mechanism of malachite green adsorption on activated carbon prepared from bamboo by K_2CO_3 activation and subsequent gasification with CO_2, J. Hazard. Mater., 157 (2008) 344–351.
[5] V. Gupta, I. Ali, D. Mohan, Equilibrium uptake and sorption dynamics for the removal of a basic dye (basic red) using low-cost adsorbents, J. Colloid Interf. Sci., 265 (2003) 257–264.
[6] H. Chen, J. Zhao, Adsorption study for removal of Congo red anionic dye using organo-attapulgite, Adsorption, 15 (2009) 381–389.
[7] I.D. Mall, V.C. Srivastava, N.K. Agarwal, I.M. Mishra, Removal of congo red from aqueous solution by bagasse fly ash and activated carbon: kinetic study and equilibrium isotherm analyses, Chemosphere, 61 (2005) 492–501.
[8] M. Kornaros, G. Lyberatos, Biological treatment of wastewaters from a dye manufacturing company using a trickling filter, J. Hazard. Mater., 136 (2006) 95–102.
[9] J.-W. Lee, S.-P. Choi, R. Thiruvenkatachari, W.-G. Shim, H. Moon, Submerged microfiltration membrane coupled with alum coagulation/powdered activated carbon adsorption for complete decolorization of reactive dyes, Water Res., 40 (2006) 435–444.
[10] H. Selcuk, Decolorization and detoxification of textile wastewater by ozonation and coagulation processes, Dyes Pigm., 64 (2005) 217–222.
[11] K. Dutta, S. Mukhopadhyay, S. Bhattacharjee, B. Chaudhuri, Chemical oxidation of methylene blue using a Fenton-like reaction, J. Hazard. Mater., 84 (2001) 57–71.
[12] M. Buonomenna, A. Gordano, G. Golemme, E. Drioli, Preparation, characterization and use of PEEKWC nanofiltration membranes for removal of Azur B dye from aqueous media, React. Funct. Polym., 69 (2009) 259–263.
[13] C.-H. Liu, J.-S. Wu, H.-C. Chiu, S.-Y. Suen, K.H. Chu, Removal of anionic reactive dyes from water using anion exchange membranes as adsorbers, Water Res., 41 (2007) 1491–1500.
[14] M. Muruganandham, M. Swaminathan, TiO_2–UV photocatalytic oxidation of Reactive Yellow 14: effect of operational parameters, J. Hazard. Mater., 135 (2006) 78–86.
[15] M. Arami, N.Y. Limaee, N.M. Mahmoodi, N.S. Tabrizi, Equilibrium and kinetics studies for the adsorption of direct and acid dyes from aqueous solution by soy meal hull, J. Hazard. Mater., 135 (2006) 171–179.
[16] S. Dawood, T.K. Sen, Removal of anionic dye Congo red from aqueous solution by raw pine and acid-treated pine cone powder as adsorbent: equilibrium, thermodynamic, kinetics, mechanism and process design, Water Res., 46 (2012) 1933–1946.
[17] Y.C. Sharma, Uma, Optimization of parameters for adsorption of methylene blue on a low-cost activated carbon, J. Chem. Eng. Data, 55 (2010) 435–439.
[18] S. Wang, Z.H. Zhu, A. Coomes, F. Haghseresht, G.Q. Lu, The physical and surface chemical characteristics of activated carbons and the adsorption of methylene blue from wastewater, J. Coll. Interf. Sci., 284 (2005) 440–446.
[19] M.T. Yagub, T.K. Sen, S. Afroze, H.M. Ang, Dye and its removal from aqueous solution by adsorption: A review, Adv. Coll. Interf. Sci., 209 (2014) 172–184.
[20] Y.-F. Lin, H.-W. Chen, P.-S. Chien, C.-S. Chiou, C.-C. Liu, Application of bifunctional magnetic adsorbent to adsorb metal cations and anionic dyes in aqueous solution, J. Hazard. Mater., 185 (2011) 1124–1130.
[21] M.U. Dural, L. Cavas, S.K. Papageorgiou, F.K. Katsaros, Methylene blue adsorption on activated carbon prepared from

Posidonia oceanica (L.) dead leaves: Kinetics and equilibrium studies, Chem. Eng. J., 168 (2011) 77–85.
[22] S. Xiao, M. Shen, R. Guo, Q. Huang, S. Wang, X. Shi, Fabrication of multiwalled carbon nanotube-reinforced electrospun polymer nanofibers containing zero-valent iron nanoparticles for environmental applications, J. Mater. Chem., 20 (2010) 5700–5708.
[23] D. Wesenberg, I. Kyriakides, S.N. Agathos, White-rot fungi and their enzymes for the treatment of industrial dye effluents, Biotechnol. Adv., 22 (2003) 161–187.
[24] J.-S. Wu, C.-H. Liu, K.H. Chu, S.-Y. Suen, Removal of cationic dye methyl violet 2B from water by cation exchange membranes, J. Membr. Sci., 309 (2008) 239–245.
[25] H.-C. Chiu, C.-H. Liu, S.-C. Chen, S.-Y. Suen, Adsorptive removal of anionic dye by inorganic–organic hybrid anion-exchange membranes, J. Membr. Sci., 337 (2009) 282–290.
[26] M.I. Khan, S. Akhtar, S. Zafar, A. Shaheen, M.A. Khan, R. Luque, Removal of Congo Red from Aqueous solution by anion exchange membrane (EBTAC): adsorption kinetics and themodynamics, Mater., 8 (2015) 4147–4161.
[27] M.I. Khan, L. Wu, A.N. Mondal, Z. Yao, L. Ge, T. Xu, Adsorption of methyl orange from aqueous solution on anion exchange membranes: Adsorption kinetics and equilibrium, Membr. Wat. Treat., 7 (2016) 23–38.
[28] R. Han, D. Ding, Y. Xu, W. Zou, Y. Wang, Y. Li, L. Zou, Use of rice husk for the adsorption of congo red from aqueous solution in column mode, Bioresour. Technol., 99 (2008) 2938–2946.
[29] S. Chatterjee, M.W. Lee, S.H. Woo, Adsorption of congo red by chitosan hydrogel beads impregnated with carbon nanotubes, Bioresour. Technol., 101 (2010) 1800–1806.
[30] Z. Hu, H. Chen, F. Ji, S. Yuan, Removal of Congo Red from aqueous solution by cattail root, J. Hazard. Mater., 173 (2010) 292–297.
[31] M.A. Shouman, N.A. Fathy, S.M. El-Khouly, A.A. Attia, Equilibrium, kinetic and thermodynamic studies of the adsorption of acidic dye onto bagasse fly ash, Carb. lett., 12 (2011) 143–151.
[32] A.-M.A.K. Salman, J.M. Abd-Hussian, N.A. Mustafa, S.A., The use of grinded white kidney beans to remove the congo red dye from aqueous solutions by adsorption, Meso. Environ. J., 3 (2017) 35–39.
[33] A. Tor, Y. Cengeloglu, Removal of congo red from aqueous solution by adsorption onto acid activated red mud, J. Hazard. Mater., 138 (2006) 409–415.
[34] F.A. Pavan, S.L.P. Dias, E.C. Lima, E.V. Benvenutti, Removal of Congo red from aqueous solution by aniline propylsilica xerogel, Dyes Pigm., 76 (2008) 64–69.
[35] T.K. Roy, N.K. Mondal, Biosorption of Congo Red from aqueous solution onto burned root of Eichhornia crassipes biomass, Appl. Wat. Sci., 7 (2017) 1841–1854.
[36] A.T. Ojedokun, O.S. Bello, Kinetic modeling of liquid-phase adsorption of Congo red dye using guava leaf-based activated carbon, Appl. Wat. Sci., 7 (2017) 1965–1977.
[37] J. Pal, M.K. Deb, Efficient adsorption of congo red dye from aqueous solution using green synthesized coinage nanoparticles coated activated carbon beads, Appl. Nanosci., 4 (2014) 967–978.
[38] C. Wu, Y. Wu, J. Luo, T. Xu, Y. Fu, Anion exchange hybrid membranes from PVA and multi-alkoxy silicon copolymer tailored for diffusion dialysis process, J. Membr. Sci., 356 (2010) 96–104.
[39] Y. Li, T. Xu, M. Gong, Fundamental studies of a new series of anion exchange membranes: membranes prepared from bromomethylated poly (2, 6-dimethyl-1, 4-phenylene oxide) (BPPO) and pyridine, J. Membr. Sci., 279 (2006) 200–208.
[40] X. Lin, L. Wu, Y. Liu, A.L. Ong, S.D. Poynton, J.R. Varcoe, T. Xu, Alkali resistant and conductive guanidinium-based anion-exchange membranes for alkaline polymer electrolyte fuel cells, J. Power Sour., 217 (2012) 373–380.
[41] L. Marçal, E. De Faria, M. Saltarelli, P. Calefi, E. Nassar, K. Ciuffi, R. Trujillano, M. Vicente, S. Korili, A. Gil, Amine-functionalized titanosilicates prepared by the sol–gel process as adsorbents of the azo-dye orange II, Ind. Eng. Chem. Res., 50 (2010) 239–246.
[42] H.A. Chanzu, J.M. Onyari, P.M. Shiundu, Biosorption of malachite green from aqueous solutions onto polylactide/spent brewery grains films: kinetic and equilibrium studies, J. Polym. Environ., 20 (2012) 665–672.
[43] M. Mohammad, S. Maitra, N. Ahmad, A. Bustam, T.K. Sen, B.K. Dutta, Metal ion removal from aqueous solution using physic seed hull, J. Hazard. Mater., 179 (2010) 363–372.
[44] F. Arias, T.K. Sen, Removal of zinc metal ion (Zn^{2+}) from its aqueous solution by kaolin clay mineral: A kinetic and equilibrium study, Coll. Surf. A: Physicochem. Eng. Asp., 348 (2009) 100–108.
[45] T.K. Sen, M.V. Sarzali, Removal of cadmium metal ion (Cd^{2+}) from its aqueous solution by aluminium oxide (Al_2O_3): A kinetic and equilibrium study, Chem. Eng. J., 142 (2008) 256–262.
[46] S. Mohan, R. Gandhimathi, Removal of heavy metal ions from municipal solid waste leachate using coal fly ash as an adsorbent, J. Hazard. Mater., 169 (2009) 351–359.
[47] P. Luo, Y. Zhao, B. Zhang, J. Liu, Y. Yang, J. Liu, Study on the adsorption of Neutral Red from aqueous solution onto halloysite nanotubes, Water Res., 44 (2010) 1489–1497.
[48] A. Roy, S. Chakraborty, S.P. Kundu, B. Adhikari, S. Majumder, Adsorption of anionic-azo dye from aqueous solution by lignocellulose-biomass jute fiber: equilibrium, kinetics, and thermodynamics study, Ind. Eng. Chem. Res., 51 (2012) 12095–12106.
[49] S. Largergren, Zur theorie der sogenannten adsorption geloster stoffe. Kungliga Svenska Vetenskapsakademiens, Handlingar 24 (1898) 1–39.
[50] N. Kannan, M.M. Sundaram, Kinetics and mechanism of removal of methylene blue by adsorption on various carbons—a comparative study, Dyes Pigm., 51 (2001) 25–40.
[51] Y.-S. Ho, Second-order kinetic model for the sorption of cadmium onto tree fern: A comparison of linear and non-linear methods, Water Res., 40 (2006) 119–125.
[52] M. Özacar, İ.A. Şengil, A kinetic study of metal complex dye sorption onto pine sawdust, Proc. Biochem., 40 (2005) 565–572.
[53] S. Chowdhury, R. Mishra, P. Saha, P. Kushwaha, Adsorption thermodynamics, kinetics and isosteric heat of adsorption of malachite green onto chemically modified rice husk, Desalination, 265 (2011) 159–168.
[54] S. Kuo, E. Lotse, Kinetics of phosphate adsorption and desorption by hematite and gibbsite 1, Soil Sci., 116 (1973) 400–406.
[55] C. Aharoni, M. Ungarish, Kinetics of activated chemisorption. Part 2.—Theoretical models, J. Chem. Soc., Faraday Trans. 1: Phys. Chem. Cond. Phas., 73 (1977) 456–464.
[56] E. Tütem, R. Apak, Ç.F. Ünal, Adsorptive removal of chlorophenols from water by bituminous shale, Water Res., 32 (1998) 2315–2324.
[57] I.D. Mall, V.C. Srivastava, N.K. Agarwal, I.M. Mishra, Adsorptive removal of malachite green dye from aqueous solution by bagasse fly ash and activated carbon-kinetic study and equilibrium isotherm analyses, Coll. Surf. A: Physicochem. Eng. Asp., 264 (2005) 17–28.
[58] B. Royer, N.F. Cardoso, E.C. Lima, J.C. Vaghetti, N.M. Simon, T. Calvete, R.C. Veses, Applications of Brazilian pine-fruit shell in natural and carbonized forms as adsorbents to removal of methylene blue from aqueous solutions—Kinetic and equilibrium study, J. Hazard. Mater., 164 (2009) 1213–1222.
[59] S. Zakhama, H. Dhaouadi, F. M'henni, Nonlinear modelisation of heavy metal removal from aqueous solution using Ulva lactuca algae, Biores. Technol., 102 (2011) 786–796.
[60] H. Dhaouadi, F. M'Henni, Vat dye sorption onto crude dehydrated sewage sludge, J. Hazard. Mater., 164 (2009) 448–458.
[61] S. Zafar, N. Khalid, M. Daud, M. Mirza, Kinetic studies of the adsorption of thorium ions onto rice husk from aqueous media: linear and nonlinear approach, Nucleus, 52 (2015) 14–19.
[62] M.C. Ncibi, Applicability of some statistical tools to predict optimum adsorption isotherm after linear and non-linear regression analysis, J. Hazard. Mater., 153 (2008) 207–212.
[63] I. Langmuir, The constitution and fundamental properties of solids and liquids. II. Liquids. 1, J. Am. Chem. Soc., 39 (1917) 1848–1906.

[64] H. Freundlich, Over the adsorption in solution, J. Phys. Chem., 57 (1906) 1100–1107.
[65] S. Chen, Q. Yue, B. Gao, Q. Li, X. Xu, Removal of Cr (VI) from aqueous solution using modified corn stalks: Characteristic, equilibrium, kinetic and thermodynamic study, Chem. Eng. J., 168 (2011) 909–917.
[66] R. Donat, A. Akdogan, E. Erdem, H. Cetisli, Thermodynamics of Pb^{2+} and Ni^{2+} adsorption onto natural bentonite from aqueous solutions, J. Coll. Interf. Sci., 286 (2005) 43–52.
[67] B. Hu, H. Luo, H. Chen, T. Dong, Adsorption of chromate and para-nitrochlorobenzene on inorganic–organic montmorillonite, Appl. Clay Sci., 51 (2011) 198–201.
[68] J.U.K. Oubagaranadin, Z. Murthy, Isotherm modeling and batch adsorbed design for the adsorption of Cu (II) on a clay containing montmorillonite, Appl. Clay Sci., 50 (2010) 409–413.
[69] O. Redlich, D.L. Peterson, A useful adsorption isotherm, J. Phys. Chem., 63 (1959) 1024–1024.
[70] M. Brdar, M. Šćiban, A. Takači, T. Došenović, Comparison of two and three parameters adsorption isotherm for Cr (VI) onto Kraft lignin, Chem. Eng. J., 183 (2012) 108–111.
[71] K. Foo, B. Hameed, Insights into the modeling of adsorption isotherm systems, Chem. Eng. J., 156 (2010) 2–10.
[72] R. Sips, Combined form of Langmuir and Freundlich equations, J. Chem. Phys., 16 (1948) 490–495.
[73] J. Liu, J. Si, Q. Zhang, J. Zheng, C. Han, G. Shao, Preparation of negatively charged hybrid adsorbents and their applications for Pb^{2+} removal, Ind. Eng. Chem. Res., 50 (2011) 8645–8657.